

Abstract — The use of array antennas in mobile telecommunication systems has proven to increase the spectral efficiency in the system. However, the use of an N element array antenna at the basestation site implies that the amount of radio hardware must be increased N -fold. This will make basestations larger, more expensive and more power consuming. Much effort must be put into combine functionality as amplification into one device, using a multicarrier amplifier (MCPA), capable to amplify a number of signals with different carrier frequencies in a single device.

In this study we investigate by measurements and simulations the effect of a nonlinearity in the MCPA:s in the downlink for a cellular system. The nonlinearity will introduce intermodulation distortion and also decrease the null-depth of the beamformer. This will have an impact on the carrier-to-interference ratio of the mobiles in the system. The simulations gives the CDF of the received carrier-to-interference ratio of the mobiles, which can be used in link budget analysis. The transmitted intermodulation distortion from an array will be spatially dispersed. This is shown by measurements in an anechoic chamber on a four element array using an analog Butler matrix as a beamformer.

I. INTRODUCTION

Introducing antenna arrays at the basestation site increases the size of the basestations by multiplication of the number of radio modems, amplifiers and so on. Simply, if a basestation is operating on M frequency channels, it needs M radio modems and M amplifiers if the conventional single carrier amplifier (SCPA) technology is applied. And by introducing an N element array antenna, the number of amplifiers increases to NM . Thus, it is highly desirable to integrate the hardware used at the base station site to reduce cost, power dissipation and the space a basestation site occupies. One proposed solution is to combine the signals prior to amplification and co-amplify them in a Multi-Carrier Power Amplifier (MCPA). Hereby, the number of amplifiers are reduced to N and no need for bulky filter combiners are needed.

When several constant-envelope signals are combined as when using the MCPA, the envelope of the composite signal becomes non-constant and the amplifier cannot be operated in the high-efficient nonlinear region of the amplifier due to the generation of intermodulation distortion. The amplifier must thus be linearized to increase its efficiency. The linearisation of MCPA:s has been the subject of considerable research effort. The combining of several independent signals give rise to a large peak-to-mean ratio of the MCPA

input signal. Even if it is possible to construct an MCPA which meets the stringent linearity requirements, its peak power requirement is much greater than the individual power of the M carriers. For example, a 16 channel basestation running 10 Watts per channel, the peak power in the MCPA could be as high as 2.56 kW [1]. The amplifier has to be biased with a large back-off from the saturating point to avoid that the peak power rating of the MCPA is exceeded. Consequently, a large back-off implies low power added efficiency (PAE), so most of the DC power is lost as heat.

The input back-off (IBO) and the output back-off (OBO) per carrier of an amplifier is defined in dB as

$$IBO = 10 \log_{10} \left(\frac{P_{sat,in}}{P_{avg,in}} \right) \quad (1)$$

$$OBO = 10 \log_{10} \left(\frac{P_{sat,out}}{P_{avg,out}} \right) \quad (2)$$

where $P_{avg,in}, P_{avg,out}$ is the average input/output power per carrier and $P_{sat,in}, P_{sat,out}$ is the input power when the output power is saturated and the corresponding output power. Nonlinearities in communication systems are commonly characterized by the amplitude to amplitude modulation (AM/AM) distortion characteristics and amplitude to phase modulation (AM/PM) distortion characteristics, which is the input amplitude dependent gain and phase conversion of the amplifier. We present a parametric model for these characterizing functions, so different degrees of nonlinearity can be studied by varying a single parameter.

When simulating multicarrier communication systems operating over nonlinear channels, the required sampling rate contributes significantly to long execution times. When the sub-carriers have constant envelopes and the number of carriers is large, the intermodulation distortion is often modeled by an additive Gaussian noise source [2]. In smart antennas, the signals that enters the MCPA has a time varying envelope, due to weight adaption and this will make the signals correlated with each other and with the intermodulation products. To simulate this, the sampling rate must be extremely high and the executing time becomes very long.

Schneider et.al. [2] presented a method to simulate a multicarrier digital communication system over a band-limited channel with a nonlinear device. The method is based on Shimbo's work [3] and reduces the simulation time significantly by only considering the intermodulation products that falls in the bandwidth of the observed sub-carriers. The simulation method is applied in this paper to evaluate the impact of nonlinearities on adaptive antenna system performance.

By introducing MCPA:s in adaptive antenna array systems, and assuming that they are not perfectly linearized, three effects can be observed:

1. Intermodulation distortion power will be emitted from the basestation. As opposed to a conventional (one-antenna) basestation, the array antenna makes the intermodulation distortion to be dependent on the azimuthal angle. Thus in some direction the intermodulation products from some or all antennas adds coherently and a mobile on that frequency and in that particular direction will experience a raised interference level. This has previously been studied by Litva [4] for receiving arrays, where the concept *phantom-lobes* were introduced.
2. The AM/AM and AM/PM conversion in the MCPA will make the transmitting antenna branches unmatched, due to phase shifts and gain compression. Thus the resulting radiation pattern will be distorted, and an intended “null” in the radiation pattern towards a known co-channel user will be shifted, and the interference for that particular user will increase.
3. Due to the large amplitude variations (Crest Factor) of the combined signal on the input of the MCPA, the peak-to-mean ratio of the input signal is often limited prior to amplification, so the peak power rating of the amplifier can be reduced. This leads to considerable benefits in terms of power and cost savings in the design of the MCPA. The limiter will also generate intermodulation products, that will be transmitted in some direction, dependent on the weight settings for that particular beam. And consequently, the signal to interference level for the mobiles will increase.

II. BASIC CONSIDERATIONS

A. Downlink transmission

The basic operation of an adaptive antenna array at a base station is to enhance the received signal by suppressing interferers transmitting on the same channel and optimally combine the signals to reduce multipath fading. The transmitter architecture is shown in Fig. 1. The receiver estimates the radio channel and performs a spatio-temporal equalization. Due to the low correlation between the uplink and downlink channel in frequency division duplex (FDD) systems [5], downlink beamforming has to be based on other information than the estimated uplink channel. This study considers a FDD system, which is a very common duplex method (GSM, AMPS, IS54, IS136, IS95 are all FDD systems). If the angular spread of the signal is small, then the spatial signature of the channel will be approximately reciprocal where the spatial signature is characterized as the direction of arrival (DOA), angular spread and power of the received signals as seen from the basestation array antenna. This information is used in calculating the downlink beamforming weights. The downlink algorithm is described in [5] and is based on the solution of a generalized eigenvalue equation.

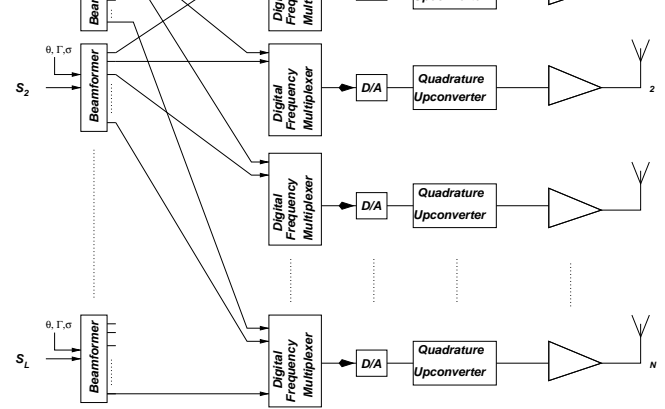


Fig. 1: Downlink adaptive antenna architecture

III. THE MULTICARRIER SIGNAL

The multicarrier signal at the amplifier input at antenna branch n can be written as:

$$x_n(t) = \operatorname{Re} \left\{ \sum_{i=1}^M w_{ni} \gamma_i s_i(t) e^{j(\omega_c + \omega_i)t} \right\} \quad (3)$$

where w_{ni} is the complex weight for signal i at antenna n and $s_i(t)$ is the i th complex information signal. The gain factor γ_i is dependent on and controlled by the downlink power control algorithm. We assume in our simulations that the power control is implemented so the transmitted power from the array gives the received power at the mobile equal to the received power at the basestation from that particular mobile. If an array antenna is used, the transmitted power per antenna is the total transmitted power divided by the number of antennas N . Thus, the amplification is distributed over several amplifiers, which shows to be beneficial in terms of peak power requirements and generated intermodulation distortion. The weights and the gain factor are assumed constant under the time period of study.

IV. A NONLINEAR POWER AMPLIFIER MODEL

In this section we introduce a memoryless model for the nonlinear power amplifier. If we express the complex envelope of the input signal as

$$z_{in}(t) = \varrho(t) \cdot e^{j\psi(t)} \quad (4)$$

then the complex envelope of the output signal can be expressed by

$$z_{out}(t) = g(\varrho(t)) e^{j(\psi(t) + f(\varrho(t)))} \quad (5)$$

where $g(\cdot)$ and $f(\cdot)$ is the AM/AM and AM/PM conversion of the nonlinear amplifier. Cann suggested a limiter model that is linear for small signals, has an asymptotic output level at large input signals and is analytic in a closed form which is desirable. Also the amplifier characteristics can be changed easily by adjusting three parameters [6]. Cann's limiter model is given as

$$g(\varrho(t)) = \frac{\nu \varrho(t)}{\left(1 + \left(\frac{\nu \varrho(t)}{K_a}\right)^s\right)^{\frac{1}{s}}} \quad (6)$$

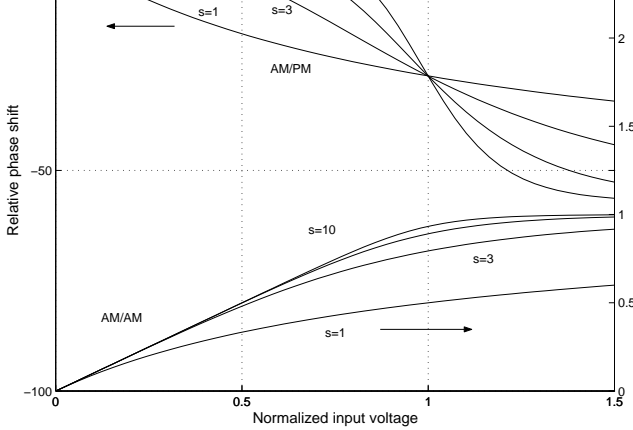


Fig. 2: Parametric AM/AM and AM/PM conversion curves

where ν is the small signal amplification (set as $\nu=1$ in the following), K_a is the output saturation level as $|\varrho(t)| \rightarrow \infty$ and s controls the knee sharpness, or the transition smoothness between the linear and nonlinear region, as seen in the lower part of Fig. 2 for different s and with $K_a=1$. The figure shows the envelope output amplitude as a function of envelope input amplitude, i.e. $g(\varrho(t))/|\varrho(t)|$ defined for a CW tone.

The AM/PM conversion for a solid state power amplifier is usually small as compared to the traveling wave tube amplifiers. At large IBO the AM/PM conversion is negligible, but when the input amplitude approaches the saturation point, the relative phase shift becomes present. This can empirically be modeled by the following expression

$$f(\varrho(t)) = \frac{K_\phi}{1 + |\varrho(t)|^s} \quad (7)$$

where K_ϕ controls the maximum AM/PM conversion in the saturation region and the parameter s is the same as for the AM/AM curves above. This leads to the upper curve family in Fig. 2, with $K_\phi=0.3$ radians.

A. Output of a multicarrier input signal from a nonlinear bandpass memoryless amplifier

To reduce simulation time we used the Shimbo Amplitude Function (SAF)-method. The work by Shimbo [3] and Schneider [2] provides the output of a bandpass memoryless nonlinear device given the nonlinearity functions $g(\cdot)$ and $f(\cdot)$, and a multicarrier input with arbitrarily amplitudes. The assumption that the memoryless amplifier is bandpass implies that only the spectral components in the first-zone, around the input frequencies are considered in the amplifier output signal. This leads to a reduction in the simulation time, because the higher order harmonics and intermodulation that falls outside the transmitter frequency band is easily removed by filtering and we avoid putting effort into representing these signals in the output signal.

From the assumption of the memorylessness, the output from amplifier n can be written as

$$y_n(t) = g[A] \cos(\omega_c t + \phi(t) + f[A]) \quad (8)$$

$\phi(t)$ depends on the amplitudes and the phases of all the M input signals. The details of the SAF-method is omitted here, the interested reader can refer to Shimbo's textbooks on the topic [7].

In the SAF-method, the expression (8) is rewritten and the SAF is introduced. The amplitude function gives the output amplitude and relative phase for any component in the output spectra (including all intermodulation products) given the input amplitudes and the AM/AM and AM/PM functions. To simplify the calculations, the AM/AM and AM/PM functions are expressed in a Bessel function series expansion. The carrier to intermodulation ratio in the output of the amplifier can then easily be calculated using the SAF.

V. THE RADIATION PATTERN

In this section the nominal radiation pattern and the radiation pattern due to intermodulation is discussed. Assuming a linear equally spaced transmitting antenna array, the received complex baseband signal at an angle θ from broadside is given by the antenna-space to beam-space transformation

$$U(\theta) = \sum_{n=1}^N \Omega_n(\theta) y_n(t) e^{-j(n-1)\frac{2\pi d}{\lambda} \sin(\theta)} \quad (9)$$

where d is the antenna element spacing, λ is the wavelength of the transmitted signal, $\Omega_n(\theta)$ is the antenna element gain for antenna n in direction θ and $y_n(t)$ is the signal transmitted from antenna n . Here we assume that the antenna elements have identical radiation patterns, thus $\Omega_n(\theta) = \Omega(\theta)$. Furthermore, the difference in λ for different carrier frequencies are neglected under the assumption that the carriers are closely spaced in frequency compared to the carrier frequency ω_c . We assume that $d = \lambda/2$ to satisfy the spatial Nyquist criterion.

We assume that a MCPA is used to amplify the multicarrier downlink signal. A simple way to create beams in the downlink is to use the butler matrix transformer. The BMT performs a linear transformation of the N input ports and has a structure similar to the fast Fourier transform [8],[9]. The N output ports are connected to the N antennas in the array. The signal at an input port p will be present at all N output ports, differing only by a phase difference $\Delta\phi_p$. The normalized input/output relationship for the BMT can thus be written as

$$x_n(t) = \frac{1}{\sqrt{N}} \sum_{p=0}^{N-1} s_p(t) e^{-jn\pi(\frac{2p}{N} - \frac{(N-1)}{N})} \quad (10)$$

where $x_n(t)$ is the output port n signal to be connected to antenna n and $s_p(t)$ is the signal connected to input port p of the BMT. The BMT performs essentially a beam-space to antenna-space transformation. The BMT can not place nulls adaptively towards interferers, it just transmits in the beam corresponding to the direction of the desired mobile. The spatial processing gain is thus dependent on the side-lobe level of the transmit radiation pattern. It is however still a candidate to downlink beamforming architecture due to its simplicity and wideband characteristics. The BMT can be

The BMT has the property that the output phase gradient is constant, that is, the phase difference between two adjacent antennas corresponding to a particular beam is a constant. This property implies that in some direction θ_{max} all the N signals are added coherently. This coherent addition is also valid for the intermodulation products, giving an increase in intermodulation power by $10\log(N)$ dB in a different direction than the direction of the desired signal (main beam). That implies that the desired user gets a reduction in intermodulation distortion power by this spatial dispersion. This have been studied for satellite mounted phased arrays [10], where it was shown how this intermodulation dispersion actually improved the capacity by radiating intermodulation distortion in directions where no users are situated or towards empty space.

In the general case, a more “intelligent” weighting technique might be used to create the downlink beams as in the case shown in Fig. 1. Now, coherent intermodulation from all N antennas might not add coherently in any direction, due to the non-constant phase gradient property. Conclusively: *The BMT gives the worst possible amplification of intermodulation products of $10\log_{10}(N)$ dB in some direction.*

VI. SIMULATIONS

The simulations aim to investigate the effect of using a MCPA at each transmitting antenna and how the IBO affects the carrier to interference ratio (CIR) for the mobiles in the system. It is desireable for the system-level link budget analysis to know the probability of a certain CIR level for the mobiles in the system given a certain amplifier and at a given amplifier back-off.

We assume a seven cell configuration with one center cell and the first tier of co-channel cells. Each cell is sectorized into three sectors and we assume that each sector use every frequency in the system. Uplink co-channel mobiles are assumed to be downlink co-channel mobiles and no frequency hopping or discontinuous transmission (DTX) is assumed.

Each sector base station consists of an uniform linear array with half-a-wavelength element spacing. The element radiation pattern is modeled with a $\cos^2(\theta)$ function. Each sector has three mobiles on different frequencies distributed uniformly over the area.

The path loss slope is set to 3.8 and the angular spread as seen from the array is 4° . Only one cluster of scatterers around the mobile is assumed, thus no delay spread is used in these simulations, which are intended to give link-level system results on CIR. The mobiles exhibit slow fading, lognormally distributed with a standard deviation of 6 dB and correlated between two basestations with correlation coefficient 0.5.

The simulation is carried out for three different antenna array sizes, with $N = 8, 4, 2$. The received power at the mobile is held constant for the three antenna configurations by adjusting the transmitted power. Thus changing N from 4 to 2, implies that the IBO of the amplifiers has to be decreased by 3 dB. The constant $P_{avg,out}$ used in equation (2) is estimated in a pre-run simulation.

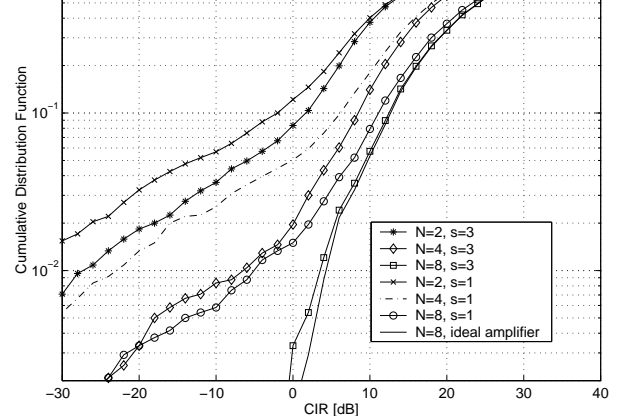


Fig. 3: Cumulative distribution function for CIR using parametric amplifier models with 12 dB OBO

It is assumed that the system is interference limited, thus the Carrier to Interferer ratio (CIR) is the quantity used for comparisons.

The total interference experienced by the test mobile is the sum of direct interference plus intermodulation from neighboring basestations. These interference sources are weighted by their respective radiation pattern and if the beamforming is optimal, the direct interference term is zero and if the amplifiers are perfectly linear, no intermodulation distortion is present. We consider only the third order intermodulation products.

VII. SIMULATION RESULTS

The cumulative distribution function (CDF) of the CIR for the test-mobile was estimated from the simulations over 800 randomized mobile positions. We investigated the impact of number of antennas in the array, the OBO and the linearity of the amplifiers. Also, the measured total degradation (TD) is defined and used to find a power efficient choice of OBO.

A. Impact of number of antennas

One important option in the design of the array is the choice of number of antennas. More antennas implies that narrower beams can be formed and more interferers can be nulled as the degrees of freedom increase. The number of antennas is limited by space and economic factors. As the amount of transceivers must be multiplied with the number of antennas, there will be a trade-off between cost and performance.

We simulated the system with $N = 2, 4$ and 8 antennas and with a moderate linear amplifier ($s = 3$) and an amplifier with poor linearity ($s = 1$). The initial OBO (for a single carrier) was chosen to 12 dB and three carriers were co-amplified in each MCPA. The OBO was adjusted to compensate for the increase in number of antennas.

The results in Fig.3 shows that when the number of antennas is increased the effect of the nonlinearity is decreased. This is due to the distribution of the amplification over several amplifiers. When the number of antennas is increased, each amplifier can be used at a larger back-off

the $s = 3$ amplifier is used in a moderately linear region. When $N = 2$ the CIR is 6 dB lower for the $s = 1$ amplifier as compared to the $s = 3$ amplifier at the CDF=5% percentile. When the number of antennas is increased to $N = 8$, this difference is reduced to 2 dB. With $N = 8$ and $s = 3$ the CDF curve is close to the ideal amplifier, thus the effect of the nonlinearity is negligible.

Another benefit of using more antennas is the increase in degrees of freedom, which can be used to create more nulls in the radiation pattern. This can be seen in Fig.3 as the difference between the curves using the same amplifier but with different number of antennas. The number of detected interferers was in the simulation 6 to 9, and with a two and a four element array it is impossible to fully suppress them all. Also the angle spread “uses up” degrees of freedom.

An interesting question is how much will the performance degrade if the OBO is decreased? Is there an optimal choice of OBO? This is investigated in the next section:

B. Choosing the Output Back-Off

We propose a method of choosing the OBO for maximal power efficiency. The idea is to study the lower tail of the probability density function for the CIR of the mobiles, e.g. the 5th or the 10th percentile of the CIR distribution. Then the degradation in CIR between a system with an ideal amplifier (perfectly linear) and this particular nonlinear amplifier at the chosen percentile is calculated. To find a reasonable choice of the OBO, we introduce the total degradation (TD) which is a useful performance measure for digital systems in the presence of nonlinearities. This parameter is defined in dB as

$$TD = \widehat{CIR} - CIR + OBO \quad (11)$$

where CIR is the upper carrier to interference ratio in dB for a given percentile with the nonlinear amplifier and \widehat{CIR} is the required carrier to interference ratio to obtain the same percentile with an perfectly linear amplifier. A good choice operation point of the systems corresponds to the minimum of equation (11) and yields a intuitively power efficient choice although no properties of optimality is claimed.

The total degradation curves for the $s = 3$ amplifier is shown in Fig. 4. At the 5th percentile the TD shows a minima when OBO=14.5 dB, 9.5 dB and 7 dB for the $N = 2, 4, 8$ antenna case respectively. At larger back-off the degradation in CIR for the mobiles is smaller, but the MCPA efficiency is lower and at smaller back-off the CIR degradation gets larger due to increase interference levels in the system from intermodulation and distorted radiation patterns.

Fig.4 shows as expected, that the eight antenna has the smallest total degradation. It will however require most DC power as we use eight amplifiers. When OBO increases, the curves approaches asymptotically the $TD=OBO$ line as the CIR approaches \widehat{CIR} . From these curves it is possible to infer a choice of OBO level for each system configuration considered.

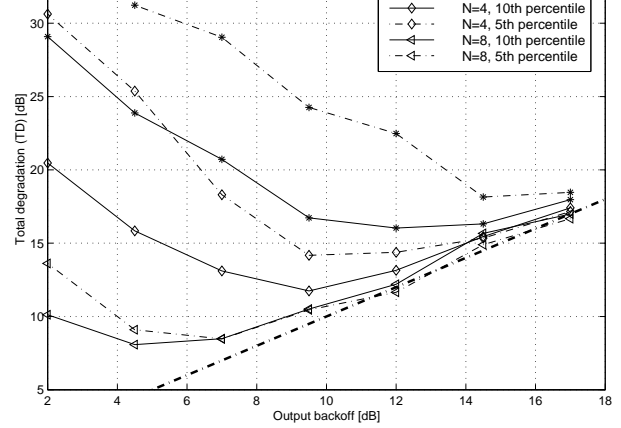


Fig. 4: Total degradation using parametric amplifier model with $s = 3$

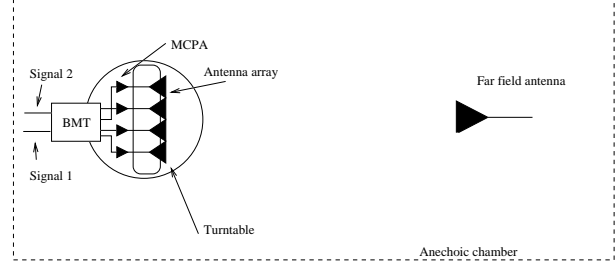


Fig. 5: Measurement setup in anechoic chamber for intermodulation measurements

VIII. MEASUREMENTS OF INTERMODULATION RADIATION PATTERNS

To verify the results of section V where a method of calculating the radiation pattern of the intermodulation distortion, measurements was performed in an anechoic chamber. We used an 4-element linear antenna array and an 8-by-8 analog BMT. Four standard microwave amplifiers was used and the setup is shown in Fig.5.

The BMT was fed with two GSM signals with center frequencies 1.8000 GHz and 1.8004 GHz in two different BMT input ports. The input power of the two signals were adjusted to the appropriate IBO and the radiation pattern was measured using the anechoic chamber with a turntable as shown in Fig.5. The angle was swept in 1° steps and for each angle the power density spectrum was measured with a spectrum analyzer.

A. Frequency-angle power spectral density measurements

These measurements gives an intuitive picture of the spatial distribution of the intermodulation distortion. Input port number 6 was used for the $f_1=1.8000$ GHz signal and port number 4 was used for the $f_2=1.8004$ GHz signal. Fig.6 and Fig.7 shows the results of the measurements. The main-lobes will, according to theory be in the directions 22.0° and -7.2° respectively, while the third order intermodulation beams would appear in direction 61° for the $2f_1 - f_2$ product at 1.7996 GHz and $2f_2 - f_1$ product at 1.8008 GHz in -39°. This is easily verified by study-

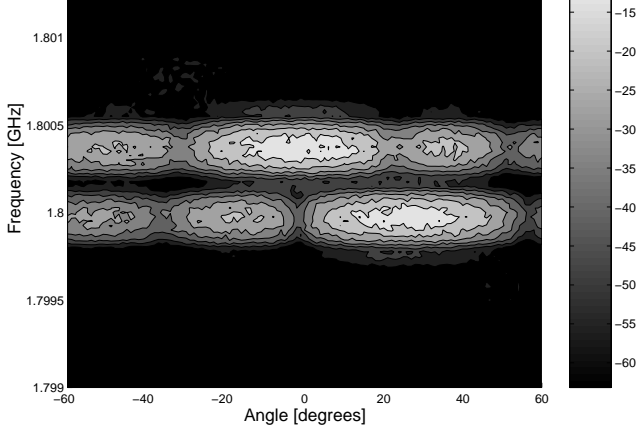


Fig. 6: Normalized frequency-angle plot of power spectral density with large back off

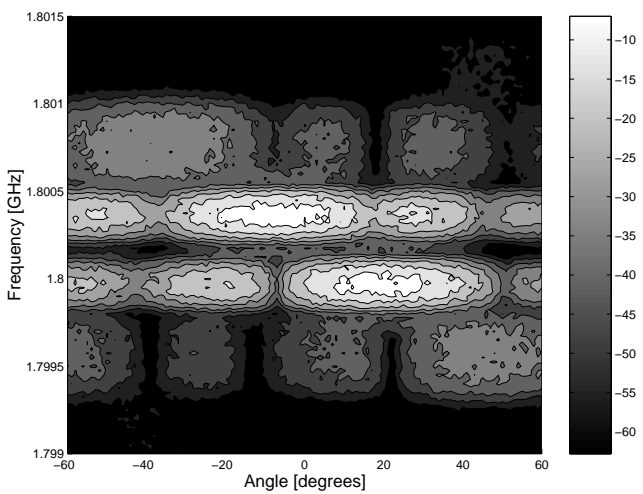


Fig. 7: Normalized frequency-angle plot of power spectral density with saturated amplifiers (input back-off decreased 8 dB compared to Fig. 6)

ing Fig.6 and Fig.7. These figures are normalized to 0dB maximum. In Fig. 7 the fifth-order intermodulation product (*e.g.* $k_1 = 3, k_2 = -2$) is weakly visible at the DOA angles 61° and -39° . Noteworthy is also the orthogonal properties of the beams from the BMT. In direction -7.2° , where beam 2 has its maxima, the other beams have nulls, giving a high level of isolation. This includes the intermodulation, which also have a null in that direction. So, by using a BMT, the spatial dimension can be used to reduce the intermodulation distortion at the mobile user. However, the IM_3 adds up coherently in another beam which increases the interference level of an eventual co-channel user that is positioned in that direction. The analog BMT used here have a manufacturing error of 0.8dB and 8.5° which spoils the orthogonality properties of the beams. These errors degrades the isolation and explains the not perfect positioned nulls in the measurements. This also demonstrate the need for calibration.

We discussed the impact of nonlinear transmit amplifiers in wireless telephone systems and concluded that the generated intermodulation distortion is generally not radiated in the same direction as the main beam. Especially for the Butler matrix beamforming network, the intermodulation and main beams are orthogonal.

By means of simulations it was shown how the CDF for the CIR of a mobile in the system is changed when the number of antennas, the degree of nonlinearity and the OBO is varied. With more antennas, the degrading effects of a nonlinear amplifier is decreased and more degrees of freedom are available to place nulls in the radiation pattern. The cost of using more antennas has to be motivated by this increase in performance. The total degradation function was introduced which has a minima corresponding to a power efficient choice of the OBO.

X. REFERENCES

- [1] P. D.W.Bennett, R.J.Wilkinson, "Determining the power rating of a multicarrier linear amplifier," *IEE Proceedings on Communications*, vol. 142, no. 4, pp. 274–280, 1995.
- [2] W. K.W. Schneider, "Efficient simulation of multicarrier digital communication systems in nonlinear channel environments," *IEEE Journal on selected areas in communications*, vol. 11, no. 3, pp. 328–339, 1993.
- [3] O.Shimbo, "Effects of intermodulation, AM-PM conversion, and additive noise in multicarrier TWT systems," *Proceedings of the IEEE*, vol. 59, no. 2, p-p. 230–239, 1971.
- [4] J.Litva and T.Lo, *Digital beamforming in wireless communications*. Boston: Artech-house Publishers, 1996.
- [5] P. Zetterberg, *Mobile Cellular Communications with Base Station Antenna Arrays: Spectrum Efficiency, Algorithms and Propagation Models*. PhD thesis, Royal Institute of Technology, Stockholm,Sweden, 1997.
- [6] A.J.Cann, "Nonlinearity model with variable knee sharpness," *IEEE Trans. on Aerospace and Electronic Systems*, vol. 16, pp. 874–878, 1980.
- [7] O. Shimbo, *Transmission analysis in communication systems, Volume 1 and 2*. Maryland,USA: Computer Science Press, 1988.
- [8] S.Drabowitch, A.Papiernik, H.Griffiths, J.Encinas, and B.L.Smith, *Modern Antennas*. Chapman and Hall, 1998.
- [9] W. Sandrin, "The butler matrix transponder," *Comsat technical review*, vol. 4, no. 2, pp. 319–345, 1974.
- [10] K. Johannsen, "Scan beam antenna intermodulation improvement due to spatial dispersion," *IEEE Transactions on Aerospace and Electronic Systems*, vol. 23, pp. 543–557, 1987.